Environ Geochem Health (2011) 33:103–112
DOI 10.1007/s10653-010-9348-0

ORIGINAL PAPER

Potential application of sludge produced from coal mine drainage treatment for removing Zn(II) in an aqueous phase

Mingcan Cui · Min Jang · Sang-Hyun Cho · Jeehyeong Khim

Received: 15 January 2010 / Accepted: 3 August 2010 / Published online: 10 November 2010

Abstract Various analyses of physico-chemical characteristics and batch tests were conducted with the sludge obtained from a full-scale electrolysis facility for treating coal mine drainage in order to find the applicability of sludge as a material for removing Zn(II) in an aqueous phase. The physico-chemical analysis results indicated that coal mine drainage sludge (CMDS) had a high specific surface area and also satisfied the standard of toxicity characteristic leaching procedure (TCLP) because the extracted concentrations of certain toxic elements such as Pb, Cu, As, Hg, Zn, and Ni were much less than their regulatory limits. The results of X-ray diffraction (XRD) and X-ray photoelectron spectroscopy (XPS) showed that the CMDS mainly consists of goethite (70%) and calcite (30%) as a weight basis. However, the zeta potential analysis represented that the CMDS had a lower isoelectric point of pH (pH_{IEP}) than that of goethite or calcite. This might have been caused by the complexation of negatively charged anions, especially sulfate, which usually exists with a high concentration in coal mine drainage. The results of Fourier transform infrared (FT-IR) spectrometry analysis revealed that Zn(II) was dominantly removed as a form of precipitation by calcite, such as smithsonite [$ZnCO_3$] or hydrozincite [$Zn_5(CO_3)_2(OH)_6$]. Recycling sludge, originally a waste material, for the removal process of Zn(II), as well as other heavy metals, could be beneficial due to its high and speedy removal capability and low economic costs.

Keywords Coal mine drainage sludge · Smithsonite · Hydrozincite · pH_{IEP} · Zn(II)

M. Cui · S.-H. Cho · J. Khim (✉)
School of Civil Environmental and Architecture Engineering, Korea University, 5 Anam-dong, Seoul 136-701, Republic of Korea
e-mail: hyeong@korea.ac.kr

M. Jang
Korea Mine Reclamation Corporation, Institute of Mine Reclamation Technology, 80-6 Coal Center, Susong-dong, , Jongno-gu, Seoul, Republic of Korea

Introduction

Acid mine drainage (AMD) could not only pollute natural environments such as surrounding soils, and surface- and groundwater, but it could also have sequential toxic effects on crops and humans through contamination (Jung 1994). The most environmentally effective techniques available for mitigating AMD are neutralization and biological processes (Watten et al. 2005). In order to select an appropriate technology for AMD, several parameters such as the chemical characteristics of the AMD, the quantity of water needed for the treatment, local climate, topographic characteristics of the on-site location and the expected life of the treatment plant should also be considered. The

chemicals usually used for neutralizing AMD include limestone, hydrated lime, soda ash, caustic soda, ammonia, calcium peroxide, kiln dust and fly ash (Watten et al. 2005; Sibrell et al. 2003). Although AMD itself could be treated by a neutralizing chemical, the chemical process usually results in the production of voluminous sludge; disposal of this sludge could create further environmental problems and additional costs. Particularly, the treatment of coal mine drainage results in a high volume of sludge because the drainage volume of coal mine is higher than that of metallic mines. In addition to the high volume of sludge, the high cost of conventional clean-up technologies for the sludge has produced economic pressure and has caused engineers to search for creative, cost-effective and environmentally sound ways to treat sludge (Bulusu et al. 2007). Compared to conventional treatment, electrolysis is a more effective method that reduces the acidity of mine drainage without using a neutralizer such as lime or limestone (Chartrand and Bunce 2003). Accordingly, as an advantage, the electrolysis process could produce a lower volume of sludge because a neutralizer is not added. Electrolysis functions with two cells (anode and cathode), in which the hydrogen ion (H^+) is reduced to H_2 in the cathode while Fe(II) is oxidized to Fe(III) in the anode. Electrolysis is known to be practical when the stoichiometric concentrations of H^+ and Fe(II) in mine drainage are nearly equivalent. In this study, the sludge produced by the electrolysis for treating coal mine drainage was designated as coal mine drainage sludge (CMDS). As an alternative of sludge treatment, the reuse of CMDS as a material in the water treatment process could be a valuable option. The following generalized mechanisms of sludge production are helpful to understand the possibility of sludge reuse as a material. Ordinarily, AMD usually contains high concentrations of sulfate and Fe(II). The CMDS that results from the treatment of coal mine drainage consists mainly of iron (oxy) hydroxide such as jarosite [$KFe_3(OH)_6(SO_4)_2$], schwertmannite [$Fe_8O_8(OH)_6SO_4$], goethite (α-FeOOH), ferrihydrite ($Fe_2O_3 \cdot 1.8\ H_2O$) or magnetite (Fe_2O_3), while containing low levels of other heavy metals (Marcello et al. 2008). As the main parameter, the pH and sulfate concentration are important to determine the identification of Fe precipitates for not only the naturally occurring sludge, but also for the sludge produced from a treatment facility. Jarosite can be formed with pH < 3 and high concentrations of sulfate, while ferrihydrite and goethite can be made at a neutral pH. Schwertmannite could be precipitated at pH $3 \sim 4$ (Jonsson et al. 2005). The structures of jarosite and schwertmannite are known to be unstable but could be transformed to more stable forms of iron precipitates such as goethite or magnetite (Jonsson et al. 2005). Accordingly, due to amorphous iron compounds, the sludge could have amphoteric characteristics of surface functional groups that can remove heavy metals (e.g. Cd, Cu, Pb, Zn) and anionic metalloids (e.g. As and Se) in an aqueous phase. However, more extensive characterization is needed to study the stability and removal mechanism for heavy metals.

In particular, the removal of heavy metals into iron compounds is thermodynamically favorable for iron compounds among other materials. For example, the adsorption of cationic heavy metal species on the hydroxyl group of goethite (α-FeOOH) has been found as an endothermic reaction. Thus, the adsorption capacities and equilibrium constants increase as the temperature increases (Angove et al. 1999; Harter 1992; Darren et al. 1993; Rodda et al. 1993, 1996a, b; Trivedi and Axe 2000). The removal of heavy metals by goethite has also been studied at various pH levels (Nita et al. 2007).

In this study, the objective is to study the possibility of sludge produced from a full-scale electrolysis process for treating coal mine drainage as a material in the field of environmental application. This is achieved through not only investigating physico-chemical properties, but also by analyzing the results of sorption isotherms and sorption kinetics, which were also compared with other referenced values of conventional media.

Materials and methods

Materials

In this study, CMDS was simply prepared by drying the sludge taken from an electrolysis treatment facility at 25°C. The facility has been operating to treat acidic mine drainage flowing from a mine edit of coal mine in Kangwon, South Korea.

Batch sorption experiments

The sorption isotherms and sorption kinetics were conducted using the suspension of CMDS in either

Table 1 AMD sampled from an abandoned gold mine and synthetic water

Item	Heavy metal (mg L^{-1})	Concentration (mg L^{-1})
AMD	Zn(II)	40
	Cu(II)	25
	Pb(II)	1.626
	Cd(II)	0.124
	As(V)	0.014
Synthetic water	Zn(II)	40

synthetic water contaminated with Zn(II) (40 mg L^{-1}) or mine drainage [main contaminants: Zn(II) (40 mg L^{-1}) and Cu(II) (25 mg L^{-1})](see Table 1) sampled from an abandoned gold mine. The obtained data of sorption isotherms and sorption kinetics were fit using the Langmuir sorption isotherm and the pseudo-second order kinetic model, respectively. The equation of the *Langmuir* sorption isotherm and pseudo-second order kinetic model was as follows:

$$q_e = \frac{bq_{\max}C_e}{1 + bC_e}$$

$$\frac{t}{q_t} = \frac{1}{k_2 q_e^2} + \frac{t}{q_e}$$

where q_e is the amount of solute adsorbed per unit weight of adsorbent (mg g^{-1}), C_e is the equilibrium concentration of solute in the bulk solution (mg L^{-1}), $q_{\max}$ is the maximum adsorption capacity (mg g^{-1}), b is the *Langmuir* constant related to the energy of adsorption, k_2 is the pseudo-second order kinetic constant, t is the time (min), q_t is the adsorbed quantity of metal ions per gram of media at any time (mg g^{-1}).

Mineralogical analysis

The particle size analysis for the sample taken from the suspension of CMDS was conducted using a particle size analyzer (LMS-300, Seishin Enterprise Co. Ltd., Tokyo, Japan) to find out whether CMDS has a seasonal variation in particle size. The elemental composition of the CMDS taken at different seasons was also determined with an X-ray fluorescence (XRF) spectrometer (XRF-1700, Shimadzu, Japan). The XRD analyses were conducted for the selected freeze-dried powdered samples of CMDS by use of a PANalytical X'Pert Pro diffract meter (fitted with an X'Celerator) with a Cu Kα radiation source at a scan speed of 2.5° min^{-1}. The phase identification of CMDS was also carried out by means of the X'Pert accompanying software program High Score Plus and the reference intensity ratio method (RIR method) ICDD PDF-4 + database (USA, 1999). Through looking at the binding energy of specific peaks, the mineral phases in the CMDS were also determined by XPS (Physical electronics PHI 5800 ESCA System), which has a monochromatic Al Kα (1486.6 eV) and anode (250W, 10kV, 27mA) X-ray source. The specific surface area of CMDS was analyzed by the Brunauer-Emmett-Teller (BET, ASAP 2010, micromeritics Inc., USA) adsorption method, which uses nitrogen gas (Quanta chrome Instruments, Sutosorb-1-C Chemisorptions- Physisorption Analyzer). The pH of CMDS was measured by the EPA method 9045c after preparing a suspension (L/S = 1:1) with distilled (DI) water. The pH of suspension was measured with a pH meter (Thermo Orion model $420A^{+}$). Heavy metals in solution were analyzed by Inductively Coupled Plasma Atomic Emission Spectrometer (ICP-AES, 5300DV, Perkin Elmer, CETA, USA). The pH_{IEP} of CMDS was found using a Zeta Meter (Zeta Meter Inc., Model 3.0+, USA), and the toxicity characteristic leaching procedure (TCLP) for CMDS was conducted by EPA method 1311, respectively. Specifically, the purpose of TCLP was to find out the stability of CMDS through analyzing the extracted toxic elements such as Pb, Cu, As, Hg, Zn, and Ni. Further mineralogical analyses were performed on gold-coated samples by a SEM (JSM 5800LV, JEOL, Japan) associated with an energy dispersive X-ray system (EDS, Link AN 10/55S). The FT-IR absorption spectra of the samples in the 400 ~ 4,000 cm^{-1} spectral range were obtained with a FT-IR spectrometer (FT-IR 6200, JASCO, USA). The IR absorption measurements were done using the KBr pellet technique. In order to obtain good quality spectra, the samples were crushed in an agate mortar and micro-size particles were obtained for FT-IR analysis.

Results and discussion

Particle size distribution of CMDS sampled at different seasons and other physico-chemical characteristics of CMDS

The particle size distribution of CMDS sampled at different seasons was shown in Fig. 1. Average

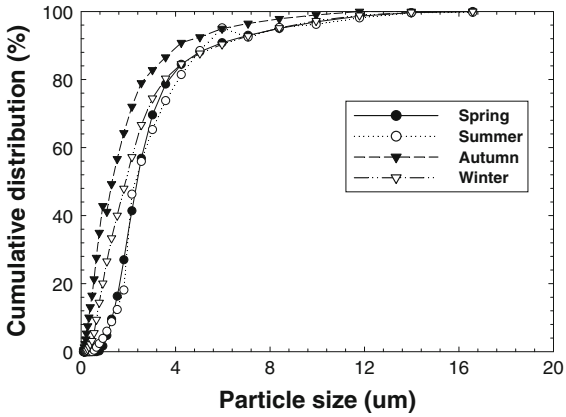

Fig. 1 Particle size distribution of the plain CMDS obtained at different seasons

particle sizes (d_{50}) for CMDS samples taken in spring, summer, autumn, and winter were 2.356, 3.310, 1.061, and 1.884 μm, respectively, representing comparably homogeneous size of particles regardless of season. Accordingly, it is not plausible that the difference in size of CMDS affects the performance of Zn(II) removal. More investigation was conducted to find the difference in chemical properties of CMDS sampled at different seasons, revealing that the seasonal variation did not affect the composition of main minerals. The average (±standard deviation) of Fe (as Fe_2O_3) and Ca (CaO) were 65(±3.03) and 9.66(±0.94)%, respectively. As minor species, the concentrations of toxic metals such as Zn (as ZnO), Ni (as NiO), Pb (as PbO), Cd (as CdO) and As (as As_2O_5) were 0.03 ~ 0.06, 0.02 ~ 0.04, 0.01 ~ 0.05, 0.01 and 0.02 ~ 0.07%, respectively, showing fairly low contents (see Table 2).

The analytical results showed that there was no any significant difference in the physico-chemical properties for CMDS sampled at different seasons (Table 2). The most interesting aspect in this analysis is that the average pore sizes of CMDS were in the range of mesopore. Porous materials can be classified by the International Union of Pure and Applied Chemistry (IUPAC) as follows: microporous (<2.0 nm), mesoporous (2.0 ~ 50.0 nm), and macroporous (>50.0 nm) (Singh et al. 1985). Macroporous materials are restricted to be used as adsorbents due to their non-uniformity of pore size distribution and low surface area. Microporous materials have limits of accessibility to active surface area due to potential blockage. Regardless of season, the measured pore size (74.42 ~ 74.98 Å) of CMDS was in the range of mesopore, which could have a low diffusion limit. As explained in physical aspects, therefore, an adsorption material developed well with mesopores could have faster sorption kinetics since adsorbate could easily adsorb on the adsorption sites. As the adsorption media have a faster sorption speed, the reactor volume and media mass could be reduced. Accordingly, the cost of the life cycle for the applied media could also be reduced to have an effective

Table 2 Physico-chemical properties of CMDS sampled at different seasons

Bulk chemistry	CMDS			
	Winter	Spring	Summer	Autumn
Major elements (%)-XRF				
SiO_2	0.24	1.03	5.56	6.65
Al_2O_3	0.57	0.79	2.55	0.52
Fe_2O_3	68.7	65.3	61.3	64.7
CaO	10.5	10.4	9.13	8.6
MgO	0.56	0.47	0.58	0.32
Na_2O	0.03	0.01	0.41	0.13
K_2O	0.02	0.07	0.32	0.08
MnO	0.32	0.38	0.36	0.38
P_2O_5	0.11	0.01	0.01	0.01
ZnO	0.03	0.03	0.03	0.06
CuO	0.01	0.01	0.01	0.013
Cr_2O_3	0.03	0.03	0.04	0.03
NiO	0.02	0.03	0.02	0.04
PbO	0.05	0.01	0.01	0.01
CdO	0.01	0.01	0.01	0.01
As_2O_5	0.02	0.02	0.05	0.07
Minor elements(mg L^{-1})-TCLP				
Pb(II)	0.025	0.021	0.092	0.006
Cu(II)	0.016	0.018	0.123	0.062
As(total)	0.025	0.024	0.058	0.064
Hg(II)	ND	ND	ND	ND
Zn(II)	0.05	0.045	0.051	0.042
Ni(II)	0.03	0.021	0.02	0.03
CN^-	0.01	ND	ND	ND
Cr(total)	0.017	ND	0.005	0.008
pH	8.3	8.2	8.31	8.25
Moisture content (wt. %)	40.85	39.52	38.98	40.25
Surface area (m^2 g^{-1})	135.4	138.2	136.8	135.2
Average pore size (Å)	74.74	74.98	74.82	74.42

ND not detected (unit: mg L^{-1}), *XRF* X-ray fluorescence

treatment process. In addition to the mesopore structure, the CMDS had a comparably high BET surface area (135.2 $\sim$ 138.2 $m^2\ g^{-1}$).

TCLP leaching test of CMDS

Analytical results of TCLP leaching tests for CMDS showed that 10 parameters, including arsenic, were satisfied with the standard of TCLP. In particular, all data of Pb(II), Cu(II), As, Zn(II), Ni(II) and Cr were less than 0.1, 0.15, 0.07, 0.05, 0.03, and 0.02 mg L^{-1}, representing much lower extracted concentrations than each regulatory limit. The Hg(II) was not detected (see Table 2). Accordingly, the problems caused by the extraction of heavy metals could not be plausible when the CMDS was used as a material in the water treatment process.

XRD and other analyses

X-ray diffraction (XRD) analyses and the reference-intensity-ratio method (RIR method) ICDD PDF-4 + database resulted in CMDS mainly consisting of goethite and calcite. The composition ratio of goethite and calcite were 70 and 30% by weight, respectively (Fig. 2). In this study, the facility of the AMD treatment is a process of electrolysis, in which there is no addition of chemicals such as lime or limestone. Originally, the acid mine drainage treated in this facility contained a high concentration of calcium because it was flowing through the limestone basin, which is the main geological constituent in the studied area. The mass ratio of Fe^{3+}/Ca^{2+} in the inflow of AMD was 2.7. Because of this, it is reasonable that the CMDS contains a high portion of calcite.

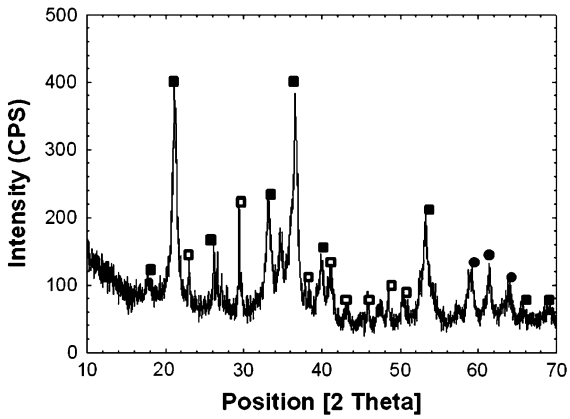

Fig. 2 XRD of CMDS [goethite (*filled square*), calcite (*empty square*), overlapped by goethite and calcite (*filled circle*)]

The XPS spectra were shown in Fig. 3. The observed binding energies (BEs) for the main Fe $2p_{3/2}$ and Ca 2p peaks of CMDS were 711.5 and 346.9 eV, respectively, falling within the range of values reported for goethite and calcite (Grosvenor et al. 2004; Abdel-Samad and Watson 1998; Garcia-Sanchez and Alvarez-Ayuso 2002). Thus, the chemical composition of CMDS might be identified as goethite and calcite. Since calcite is an insulator and samples charged during the XPS analysis, the BEs in this study were determined by aligning the C 1 s (289 eV) feature due to the CO_3^{2-} group of calcite, consistent with prior XPS studies of calcite (Baer and Moulder 1993; Stipp 1999).

Isoelectric point of pH (pH_{IEP}) of CMDS

The surface property of iron (oxy) hydroxide compounds is important for adsorbing heavy metals. The pH_{IEP} is an important index to find the status of balance between positive and negative charges on the surface of mineral. The surface functional groups $FeOH_2^+$ is the dominant species as the pH of the background aqueous phase is lower than pH_{IEP}, whereas FeO^- is dominant when the pH is higher than pH_{IEP}.

$$\mathrm{pH} < \mathrm{pH_{PZC}} : \mathrm{FeOH} + \mathrm{H^+} \leftrightarrow \mathrm{FeOH_2^+} \quad (\log k + 7.29)$$
$$\mathrm{pH} < \mathrm{pH_{PZC}} : \mathrm{FeOH} \leftrightarrow \mathrm{FeO^-} + \mathrm{H^+} \quad (\log k = -8.93)$$

Therefore, due to the electrostatic attraction, the removal of positively charged heavy metals could be

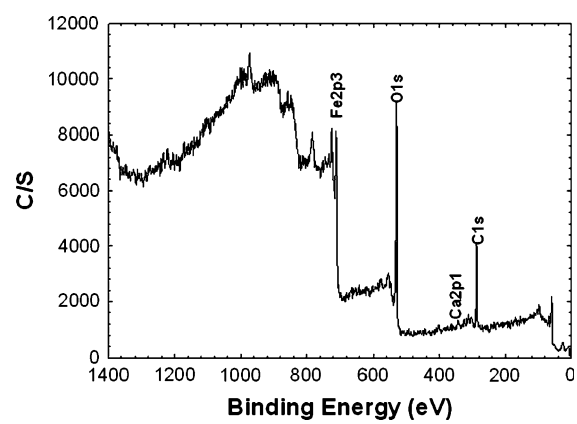

Fig. 3 XPS spectrum of plain CMDS

advantageous when the negative charge species, FeO^-, is predominant on the surface of minerals. However, this concept could be acceptable if the pure iron (oxy) hydroxide is present. Although the pH_{IEP} of goethite and $CaCO_3$ have been generally known to be 8.5 $\sim$ 9.6 and 7 $\sim$ 11, respectively (Erdemoglu et al. 2004; Kloproeeg et al. 2006; Dzombak and Morel 1990), the results of zeta potential measurement showed that the pH_{IEP} values of CMDS were 5 and 4.5 with the suspension of DI and 0.01 M NaCl, respectively (see Fig. 4). Accordingly, the pH_{IEP} of CMDS was much lower than those of goethite and $CaCO_3$, which were found to be the main components, as shown in the results of XRD and XPS. The low value of pH_{IEP} might be explained by the fact that high concentrations of negative charged anions and sulfate are incorporated in the structural networks. These are adsorbed as an outer-sphere complexation on the surface of CMDS, which was produced from the treatment of acid mine drainage of coal mine containing high level of sulfate (Swedlund and Webster 2001). In general, acid mine drainage that contains a high level of sulfate, as well as iron (oxy) hydroxyl sulfate, could be precipitated during the treatment process. However, the structures of jarosite and schwertmannite, which are usually found as the main precipitates, are not stable and could be transformed to more stable forms of iron precipitates such as goethite or magnetite (Jonsson et al. 2005). Due to this complexation of sulfate, the CMDS could develop electrostatically negative charges at a neutral pH and have more attraction for cationic heavy metals.

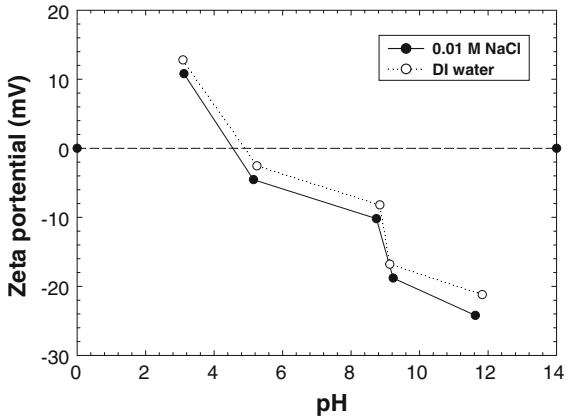

Fig. 4 Zeta potential analysis of CMDS suspended with DI and 0.01 M ionic strength with NaCl

$$FeOH_2^+ + SO_4^{2-} \leftrightarrow FeOH - SO_4^{2-} + H^+$$

Kinetics study

As shown in the high determination coefficients (more than 0.98 for all tests), the Langmuir adsorption isotherm and pseudo-second order model fit well with the adsorption isotherm (Fig. 5a) and adsorption kinetic (Fig. 5b) data of CMDS. The main reason to use simple models such as the Langmuir adsorption isotherm and pseudo-second order kinetic was to analyze the data and compare it with other referenced values obtained by conventional media. The CMDS had comparably higher sorption capacities (14.1 mg g^{-1}) of Zn(II) in synthetic water than other referenced materials (Table 3). The result of K_2 obtained by fitting the data with the pseudo-second order kinetic model was 12.1 $\times$ 10^{-2} g $mg^{-1}min^{-1}$ for the Zn(II) removal in synthetic water. As shown in the adsorption isotherm results, the comparison of rate constants also represented that the CMDS had a much faster sorption speed than those of other materials. However, the maximum adsorption capacity and rate constant for the Zn(II) removal in AMD were much lower at 4.22 mg g^{-1} and 3.0 $\times$ 10^{-2} g $mg^{-1}min^{-1}$. These results could be explained by the reason that other metal species existing in AMD such as Cu(II), Pb(II), and Cd(II) were also removed to consume the adsorption sites of CMDS. Figure 5C shows the kinetics of heavy metals removal in AMD by CMDS. Within 1 h, the concentrations of most heavy metals, except Zn(II), decreased to less than 0.01 mg L^{-1}, which was the detection limit of ICP.

Thus, we could consider that the CMDS has great potential as a material for removing heavy metals in various fields of the wastewater treatment process.

SEM–EDS analyses of Zn(II) adsorbed CMDS

Scanning electron microscopy (SEM) and energy dispersive spectrometric (EDS) analyses were conducted for the Zn(II) containing CMDS. Several observations for the surface of different particles of CMDS using SEM–EDS showed that Zn(II) was evenly distributed to CMDS and not associated with the forms of crystallized hydroxide (Fig. 6), suggesting that surface co-precipitation is to be another mechanism of Zn(II) removal (Table 4).

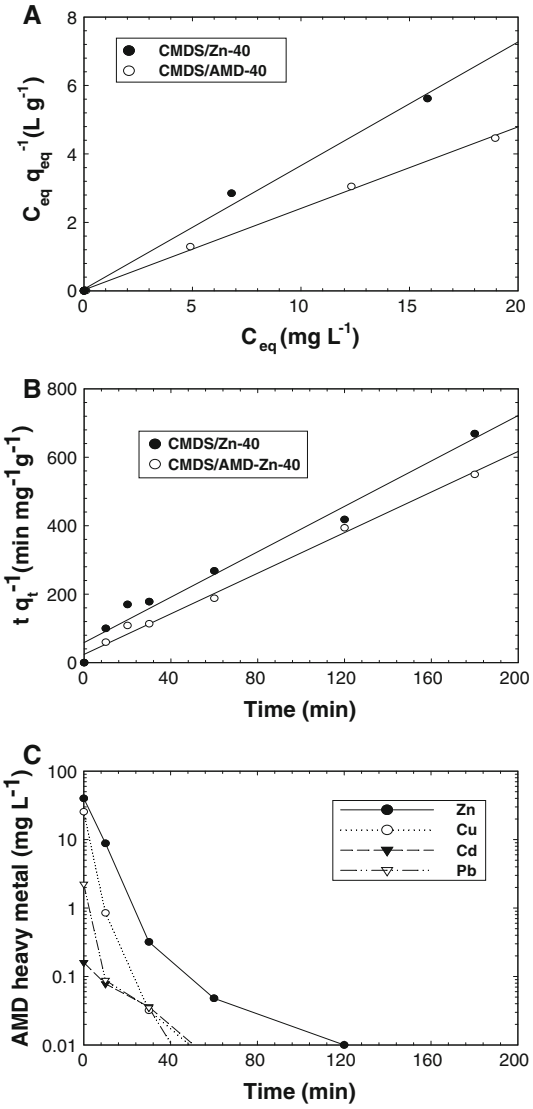

Fig. 5 **a** Zn(II) adsorption isotherms and the fit of Langmuir isotherms, **b** kinetic data and the fit of pseudo-second-order kinetic model for the suspension of CMDS with the Zn(II) contaminated synthetic water and AMD, **c** kinetic data of Cu(II), Zn(II), Cd(II) and Pb(II) (Initial Zn(II) conc. of each water sample 40 mg L^{-1}, Cu(II) 25.5 mg L^{-1}, Cd(II) 0.124 mg L^{-1} and Pb(II) 1.626 mg L^{-1}, temperature: 25°C and pH natural)

FT-IR spectroscopic analysis

The infrared spectrum for plain CMDS and Zn(II) retained CMDS was obtained in the range of 500 ~ 4,000 cm^{-1} (Fig. 7). Table 5 shows the comparison of major IR bands with other references. As the results of FT-IR analysis were compared, the following major bands of Zn(II) retained CMDS were shifted to lower wave numbers by the Zn(II) removal. The wave numbers of OH stretching and bending vibration for Zn(II) retained CMDS were reduced to 3,178 and 1,641 cm^{-1} by 3 and 8 cm^{-1}, respectively. There were two IR bends in the case of Fe-OH vibration, with which the wave numbers (882.6 and 794.5 cm^{-1}) of plain CMDS were shifted to lower numbers (877.8 and 790.3 cm^{-1}) by about 5 cm^{-1} with the Zn(II) adsorption. Compared to the major IR bends explained above, a significant change was obtained in the carbonate IR bend. When the Zn(II) was adsorbed onto the CMDS, the carbonate wave number (1366.4 cm^{-1}) for plain CMDS reduced to 1339.7 cm^{-1} by about 26 cm^{-1}. Accordingly, when considering those shifts or changes of peak for each major band, it could be plausible that the precipitation by calcite such as smithsonite [$ZnCO_3$] or hydrozincite [$Zn_5(CO_3)_2(OH)_6$] is the dominant mechanism to remove Zn(II) rather than the complexation by iron compounds (Uygur and Rimmer 2000). Although the FT-IR analysis did not detect the IR bends for sulfate, the product of $ZnSO_4$ could have resulted as another mechanism of Zn(II) removal since the negatively charged surface functional group ($–SO_4^{2-}$) analyzed in the zeta potential measurement could have an electrostatic attraction for cationic Zn(II). However, the Zn(II) might be dominantly

Table 3 Comparison of the maximum adsorption capacity (q_{max}) of Zn(II) for various sorbents including CMDS

Adsorbents	q_{max} (mg g^{-1})	b (L mg^{-1})	Reference
Modified montmorillonite	7.8	-	Lin and Juang (2002)
Goethite	3.48	0.45	Li et al. 2008
Hematite	0.91	0.43	Li et al. 2008
Natural iron powder	1.25	0.21	Li et al. 2008
Ferrihydrite	7.29	1.21	Li et al. 2008
Fly ash	5.82	0.05	Mishra and Patel (2009)
Active carbon	11.24	0.02	Mishra and Patel (2009)
Akaganeite granular	13.95	0.03	Deliyanni et al. (2007)
CMDS/Zn(II)-40	14.08	0.27	This study
CMDS/AMD-40	4.22	0.17	

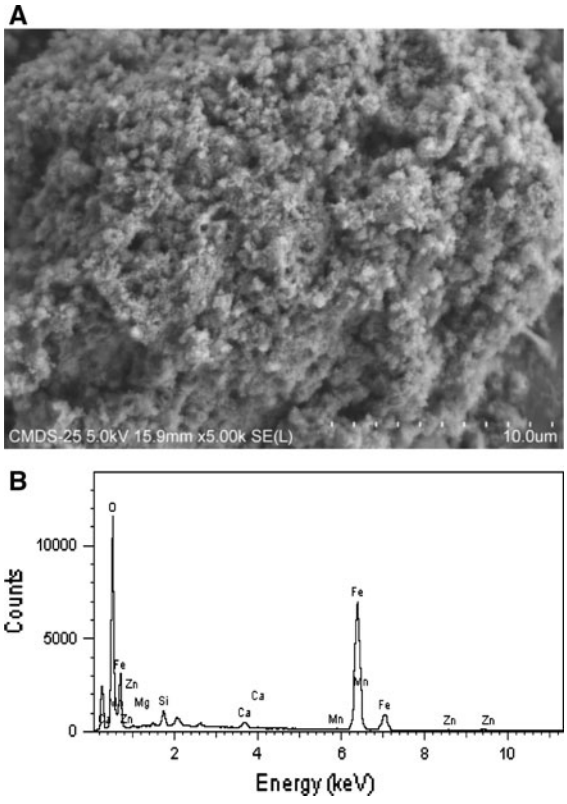

Fig. 6 SEM imaging (**a**) and EDS analysis (**b**) of Zn(II) adsorbed CMDS [Zn(II) 40 mg L^{-1}]

precipitated as carbonate compounds since the solubility product of $ZnSO_4$ ($K_{sp} = 10^{-3.01}$ as 25°C) is much higher than that of smithsonite [$ZnCO_3$ $K_{sp} = 10^{-9.82}$ as 25°C] or hydrozincite [$Zn_5(CO_3)_2(OH)_6$ $K_{sp} = 10^{-14.9}$ as 25°C] (Alwan and Williams 1979).

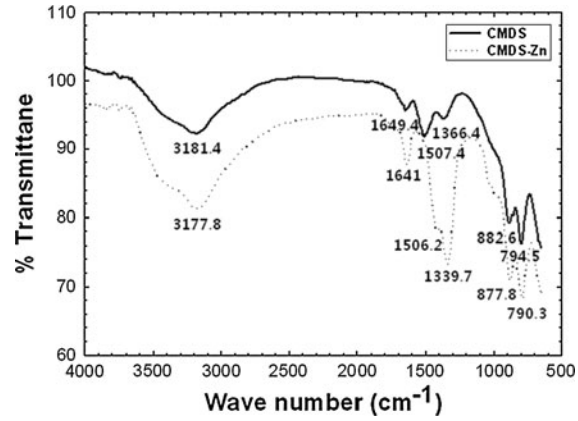

Fig. 7 FT-IR spectra of plain CMDS and Zn(II) retained CMDS [Zn(II) 40 mg L^{-1}]

Conclusions

The results of physico-chemical analysis showed that the CMDS obtained from a full-scale electrolysis process for treating coal mine drainage had a high number of specific surface areas and satisfied the standards of TCLP because all toxic heavy metals analyzed were much less than their regulatory limits. The CMDS obtained at all seasons had similar and homogeneous characteristics, while the XRD and XPS revealed that the CMDS mainly consisted of goethite and calcite. In comparison with other conventional materials, the Zn(II) removal capacities and speeds by CMDS were higher, which shows they have greater potential as an effective material in the water treatment process. Since the CMDS is a waste material originally produced from the treatment

Table 4 Rate constants and determination coefficients (R^2) of the pseudo-second order kinetic model fitting for Zn(II) adsorption data obtained with synthetic water and AMD by CMDS

Adsorbents	Temperature (K)	K_2 (g mg^{-1} min^{-1})	R^2	Reference
Crosslinked chitosan	–	0.534×10^{-2}	0.999	Chen et al. (2008)
Alginate	298	9.8×10^{-2}	0.989	Bayramouglu and Yakup Arica (2009)
Typha domingensis leaf powder	298	4.13×10^{-2}	1	Abdel-Ghani et al. (2009)
Kaolin clay	303	1.71×10^{-2}	0.998	Arias and Kanti Sen (2009)
Phosphate rock	303	0.0336×10^{-2}	0.935	Prasad et al. (2008)
Keratin powder	298	0.612×10^{-2}	0.99	Souag et al. (2009)
Plant sand	298	1.05×10^{-2}	0.99	Mohapatra et al. (2009)
CMDS/Zn(II)-40	298	12.1×10^{-2}	0.984	This study
CMDS/AMD-40	298	3.0×10^{-2}[a]	0.963	

[a] Heavy metals from natural AMD

Table 5 Frequencies (cm^{-1}) assignments for CMDS adsorption of zinc ion and literature review

IR bands	Wave number (cm^{-1})	Reference
OH-stretching vibrations mode	3,181/3,178	This study
	3,000–4,000	Kloproeeg et al. (2006); Frost et al. (2006).
	3,383	Sudakar et al. (2007)
OH-bending mode	1,649/1,641	This study
	1,600–1,700	Kloproeeg et al. (2006); Frost et al. (2006)
	1,636	Sudakar et al. (2007)
Carbonate	(1,507 and 1,366)/1,340	This study
	1,360	Jose dos Reis et al. (2004)
	1,545, 1,535 and 1,380 (hydrozincite)	Hales and Frost (2007)
Fe–O–H bending	(883 and 795)/(878 and 790)	This study
	893 and 797	Sudakar et al. (2007)
	902 and 801	Krehula et al. (2002)
Fe–O stretching vibrations	630	This study
	630, 495 and 270	Verdonck et al. (1982)

process of coal mine drainage, it could be economically applied as an advanced and effective sorption media for the removal process of heavy metals which widely exist in groundwater, AMD, industrial wastewater, etc.

Acknowledgment This study was supported by the Korea Ministry of Environment as the GAIA (Geo-Advanced Innovative Action) Project (No. 173-091-003) and a Korea University Grant.

References

Abdel-Ghani, N. T., Hegazy, A. K., & El-Chaghaby, G. A. (2009). Typha domingensis leaf powder for decontamination of aluminium, iron, zinc and lead: Biosorption kinetics and equilibrium modeling. *International Journal of Environmental Science and Technology, 6*(2), 243–248.

Abdel-Samad, H., & Watson, P. R. (1998). An XPS study of the adsorption of lead on goethite. *Surface Science, 136*, 46–54.

Alwan, A. K., & Williams, P. A. (1979). Mineral formation from aqueous solution. Part 1. The deposition of hydrozincite, $Zn_5(OH)_6(CO_3)_2$, from natural waters. *Transition Metal Chemistry, 4*, 128–132.

Angove, M. J., Wells, J. D., & Johnson, B. B. (1999). The influence of temperature on the adsorption of Cadmium (II) and Cobalt (II) on Goethite. *Journal of Colloid and Interface Science, 211*, 281–290.

Arias, F., & Kanti Sen, T. (2009). Removal of zinc metal ion from its aqueous solution by kaolin clay mineral: A kinetic and equilibrium study. *Colloids and surfaces A: Physicochemistry Engineering, 348*, 100–108.

Baer, D. R., & Moulder, J. F. (1993). High resolution XPS spectrum of calcite ($CaCO_3$,). *Surface Science Spectra, 2*, l–7.

Bayramouglu, G., & Yakup Arica, M. (2009). Construction a hybrid biosorbent using scenedesmus quadricauda and Ca-alginate for biosorption of Cu(II), Zn(II) and Ni(II): Kinetics and equilibrium studies. *Bioresourse Technology, 100*, 186–193.

Bulusu, S., Aydilek, A. H., & Rustagi, N. (2007). CCB-based encapsulation of pyrite for remediation of acid mine drainage. *Journal of Hazardous Materials, 143*(3), 609–619.

Chartrand, M. M. G., & Bunce, N. J. (2003). Electrochemical remediation of acid mine drainage. *Applied Electrochemistry, 33*, 259–264.

Chen, A. H., Liu, S. C., Chen, C. Y., & Chen, C. Y. (2008). Comparative adsorption of Cu(II), Zn(II) and Pb(II) ions in aqueous solution on the crosslinked chitosan with epichlorohydrin. *Journal of Hazardous Materials, 154*, 184–191.

Darren, P. R., Bruce, B. J., & John, D. W. (1993). The effect of temperature and pH on the adsorption of copper, Lead and Zinc onto Goethite. *Journal of Colloid and Interface Science, 161*, 57–62.

Deliyanni, E. A., Peleka, E. N., & Matis, K. A. (2007). Removal of zinc ion from water by sorption onto iron-based nano-adsorbent. *Journal of Hazardous Materials, 141*, 176–184.

Dzombak, D. A., & Morel, F. M. (1990). *Surface complexation modeling (hydrous ferric oxide)*. New York: Wiley Inter science.

Erdemoglu, N., Sahin, E., Senera, B., & Ide, S. (2004). Structural and spectroscopic characteristics of two lignans from Taxus baccata L. *Journal of Molecular Structure, 692*, 57.

Frost, R. L., Musumeci, A. W., Kloprogge, J. T., Adebajo, M. O., & Martens, W. N. (2006). Raman spectroscopy of

hydrotalcites with phosphate in the interlayer: Implications for the removal of phosphate from water. *Raman Spectroscopy, 37*(7), 733–741.

Garcia-Sanchez, A., & Alvarez-Ayuso, E. (2002). Sorption of Zn, Cd and Cr on calcite. Application to purification of industrial wastewaters. *Minerals Engineering, 15*, 539–547.

Grosvenor, A. P., Kobe, B. A., Biesinger, M. C., & Mcintyre, N. S. (2004). Investigation of multi-plet splitting of Fe 2p XPS spectra and bonding in ion compounds. *Surface and Interface Analysis, 36*, 1564–1574.

Hales, M. C., & Frost, R. L. (2007). Synthesis and vibratinal spectroscopic characterization of synthetic hydrozincite and smithsonite. *Plyhedron, 26*, 4955–4962.

Harter, R. D. (1992). Competitive sorption of Cobalt, Copper, and Nickel ions by a calcium-saturated soil. *Soil Science Society, 56*, 444–449.

Jonsson, J., Persson, P., Sjobrg, S., & Lovgren, L. (2005). Schwertmannite precipitated from acid mine drainage: Phase transformation, sulphate release and surface properties. *Applied Geochemistry, 20*, 179–191.

Jose dos Reis, M., Silverio, F., Tronto, J., & Valim, J. B. (2004). Effects of pH, temperature, and ionic strength on adsorption of sodium dodecylbenzenesulfonate into Mg-Al-CO_3^{2-} layered double hydroxides. *Physics and Chemistry of Solids, 65*, 487–492.

Jung, M. C. (1994). Sequential extraction of heavy metals in soils and a case study. *Korea Society of Economic and Environmental Geology, 27*, 469–477.

Kloproeeg, J. R., Hickey, L., Trujillano, R., Holgado, M. J., San Roma, M. S., Rives, V., et al. (2006). Characterization of intercalated Ni/Al hydrotalcites prepared by the partial decomposition of urea. *Crystal Growth & Design, 6*, 1533–1536.

Krehula, S., Popovic, S., & Music, S. (2002). Synthesis of acicular α-FeOOH particles at a very high pH. *Materials Letters, 54*, 108–113.

Li, Y., Liu, J. L., Wang, X. L., Wang, T., & Du, X. Y. (2008). Cu^{2+} and Zn^{2+} adsorption to synthetic iron oxides and natural iron ore powder. *IEEE*, 2900–2903.

Lin, S. H., & Juang, R. S. (2002). Heavy metal removal from water by sorption using surfactant-modified montmorillonite. *Journal of Hazardous Materials, B92*, 315–326.

Marcello, R. R., Galato, S., Peterson, M., Riella, H. G., & Bernardin, A. M. (2008). Inorganic pigments made from the recycling of coal mine drainage treatment sludge. *Environmental Management, 88*, 1280–1284.

Mishra, P. C., & Patel, R. K. (2009). Removal of lead and zinc ions from water by low cost adsorbents. *Journal of Hazardous Materials, 168*, 319–325.

Mohapatra, M., Khatun, S., & Anand, S. (2009). Adsorption behavior of Pb, Cd and Zn on NALCO plat sand. *Chemical Technology, 16*, 291–300.

Nita, S., Lee, Y. J., Huifang, X., et al. (2007). Ciardelli, Jean-Francois Gaillard: Role of Fe(II) and phosphate in arsenic uptake by coprecipitation. *Geochimica et Cosmochimica Acta, 71*, 3193–3210.

Prasad, M., Xu, H. Y., & Saxena, S. (2008). Multi-component sorption of Pb(II), Cu(II) and Zn(II) onto low-cost mineral adsorbent. *Journal of Hazardous Materials, 154*, 221–229.

Rodda, D. P., Johnson, B. B., & Wells, J. D. (1993). The effect of temperature and pH on the adsorption of Copper (II), Lead (II), and Zinc (II) onto goethite. *Journal of Colloid and Interface Science, 161*, 57–62.

Rodda, D. P., Johnson, B. B., & Wells, J. D. (1996a). Modeling the effect of temperature on adsorption of Lead (II) and Zinc (II) onto goethite at constant pH. *Journal of Colloid and Interface Science, 184*, 365–377.

Rodda, D. P., Wells, J. D., & Johnson, B. B. (1996b). Anomalous adsorption of Copper (II) on goethite. *Journal of Colloid and Interface Science, 184*, 564–569.

Sibrell, P. L., Watten, B. J., & Boone, T. (2003). Remediation of acid mine drainage at the Friendship Hill National Historic Site with a pulsed limestone bed process. In C. A. Young, A. M. Alfantazi, C. G. Anderson, D. B. Dreisinger, & A. James (Eds.), *Hydrometallurgy 2003* (pp. 1823–1836). Littleton, CO: The Minerals, Metals and Material Society.

Singh, Y., Stoessel, J. P., & Wolynes, P. G. (1985). Hard-sphere glass and the density-functional theory of aperiodic crystals. *Physical Review Letters, 54*, 1059–1062.

Souag, R., Touaibia, D., Benayada, B., & Boucenna, A. (2009). Adsorption of heavy metals (Cd, Zn and Pb) from water using keratin powder prepared from algerien sheep hoofs. *European Journal of Scientific Research, 35*(3), 416–425.

Stipp, S. L. S. (1999). Toward a conceptual model of the calcite surface: Hydration, hydrolysis, and surface potential. *Geochimica et Cosmochimica Acta, 63*, 3121–3131.

Sudakar, C., Kharel, P., Lawes, G., Suryanarayanan, R., Naik, R., & Naik, V. M. (2007). Raman spectroscopic studies of oxygen defects in co-doped ZnO films exhibiting room-temperature ferromagnetism. *Physics Condensed Matter, 19*, 1–9.

Swedlund, P. J., & Webster, J. G. (2001). Cu and Zn ternary surface complex formation with SO_4 on ferrihydrite and schwertmannite. *Geochemistry, 16*, 503–511.

Trivedi, P., & Axe, L. (2000). Modeling Cd and Zn sorption to hydrous metal oxides. *Environmental Science and Technology, 34*, 2215–2223.

Uygur, V., & Rimmer, D. L. (2000). Reactions of zinc with iron-oxide coated calcite surfaces at alkaline pH. *European Journal of Soil Science, 51*, 511–516.

Verdonck, L., Hoste, S., Roelandt, F. F., & Van der Kelen, G. P. (1982). Normal coordinate analysis of a-FeOOH A molecular approach. *Journal of Molecular Structure, 79*, 273–279.

Watten, B. J., Sibrell, P. L., & Schwartz, M. F. (2005). Acid neutralization within limestone sand reactors receiving coal mine drainage. *Environmental Pollution, 137*(2), 295–304.